Reactor Measurement of θ_{13} and Its Complementarity to Long-Baseline Experiments

H. Minakata,* H. Sugiyama,† and O. Yasuda‡

Department of Physics, Tokyo Metropolitan University, Hachioji, Tokyo 192-0397, Japan

K. Inoue§ and F. Suekane¶

Research Center for Neutrino Science,
Tohoku University, Sendai, Miyagi, 980-8578, Japan
(Dated: January 12, 2004)

Abstract

A possibility to measure $\sin^2 2\theta_{13}$ using reactor neutrinos is examined in detail. It is shown that the sensitivity $\sin^2 2\theta_{13} > 0.02$ can be reached with 40 ton-year data by placing identical CHOOZ-like detectors at near and far distances from a giant nuclear power plant whose total thermal energy is $24.3\,\mathrm{GW_{th}}$. It is emphasized that this measurement is free from the parameter degeneracies which occur in accelerator appearance experiments, and therefore the reactor measurement plays a role complementary to accelerator experiments. It is also shown that the reactor measurement may be able to resolve the degeneracy in θ_{23} if $\sin^2 2\theta_{13}$ and $\cos^2 2\theta_{23}$ are relatively large.

PACS numbers: 14.60.Pq,25.30.Pt,28.41.-i

*Electronic address: E-mail: minakata@phys.metro-u.ac.jp
†Electronic address: E-mail: hiroaki@phys.metro-u.ac.jp
‡Electronic address: E-mail: yasuda@phys.metro-u.ac.jp
§Electronic address: E-mail: inoue@awa.tohoku.ac.jp
¶Electronic address: E-mail: suekane@awa.tohoku.ac.jp

Typeset by REVTEX

I. INTRODUCTION

Despite the accumulating knowledges of neutrino masses and the lepton flavor mixing by the atmospheric [1], the solar [2, 3], and the accelerator [4] neutrino experiments, the (1-3) sector of the Maki-Nakagawa-Sakata (MNS) matrix [5] is still in the dark. At the moment, we only know that $|U_{e3}| = \sin\theta_{13} \equiv s_{13}$ is small, $s_{13}^2 \lesssim 0.03$, by the bound imposed by the CHOOZ reactor experiment [6]. In this paper we assume that the light neutrino sector consists of three active neutrinos only. One of the challenging goals in an attempt to explore the full structure of lepton flavor mixing would be measuring the leptonic CP or T violating phase δ in the MNS matrix. If KamLAND [7] confirms the Large-Mixing-Angle (LMA) Mikheev-Smirnov-Wolfenstein (MSW) [8, 9] solution of the solar neutrino problem, the most favored one by the recent analyses of solar neutrino data [3, 10], we will have an open route toward the goal. Yet, there might still exist the last impasse, namely the possibility of too small value of θ_{13}. Thus, it is recently emphasized more and more strongly that the crucial next step toward the goal would be the determination of θ_{13}.

In this paper, we raise the possibility that $\bar{\nu}_e$ disappearance experiment using reactor neutrinos could be potentially the fastest (and the cheapest) way to detect the effects of nonzero θ_{13}. In fact, such an experiment using the Krasnoyarsk reactor complex has been described earlier [11], in which the sensitivity to $\sin^2 2\theta_{13}$ can be as low as ~ 0.01, an order of magnitude lower than the CHOOZ experiment. We will also briefly outline basic features of our proposal, and reexamine the sensitivity to $\sin^2 2\theta_{13}$ in this paper.

It appears that the most popular way of measuring θ_{13} is the next generation long baseline (LBL) neutrino oscillation experiments, MINOS [12], OPERA [13], and the JHF phase I [14]. It may be followed either by conventional superbeam [15] experiments, the JHF phase II [14] and possibly others [16, 17], or by neutrino factories [18, 19]. It is pointed out, however, that the measurement of θ_{13} in LBL experiments with only neutrino channel (as planned in the JHF phase I) would suffer from large intrinsic uncertainties, on top of the experimental errors, due to the dependence on an unknown CP phase and the sign of Δm_{31}^2 [20]. Furthermore, it is noticed that the ambiguity remains in determination of θ_{13} and other parameters even if precise measurements of appearance probabilities in neutrino as well as antineutrino channels are carried out, the problem of the parameter degeneracy [20, 21, 22, 23, 24, 25, 26]. (For a global overview of the parameter degeneracy, see [26].) While some ideas toward a solution are proposed the problem is hard to solve experimentally and it is not likely to be resolved in the near future.

We emphasize in this paper that reactor $\bar{\nu}_e$ disappearance experiment provide particularly clean environment for the measurement of θ_{13}. Namely, it can be regarded as a dedicated experiment for determination of θ_{13}; it is insensitive to the ambiguity due to all the remaining oscillation parameters as well as to the matter effect. This is in sharp contrast with the features of LBL experiments described above. Thus, the reactor measurement of θ_{13} will provide us valuable information complementary to the one from LBL experiments and will play an important role in resolving the problem of the parameter degeneracy. It will be shown that reducing the systematic errors is crucial for the reactor measurement of θ_{13} to be competitive in accuracy with LBL experiments. We will present a preliminary analysis of its possible roles in this context. It is then natural to think about the possibility that one has better control by combining the two complementary way of measuring θ_{13}, the reactor and the accelerator methods. In fact, we will show in this paper that nontrivial relations exist between the θ_{13} measurements by both methods thanks to the complementary nature

of these two methods, so that in the luckiest case one may be able to derive constraints on the value of the CP violating phase δ, or to determine the neutrino mass hierarchy.

II.   REACTOR EXPERIMENT AS A CLEAN LABORATORY FOR θ_{13} MEASUREMENT

Let us examine in this section how clean the measurement of θ_{13} by the reactor experiments is. To define our notations, we note that the standard notation [27],

$$
U = \begin{bmatrix} c_{12}c_{13} & s_{12}c_{13} & s_{13}e^{-i\delta} \\ -s_{12}c_{23} - c_{12}s_{23}s_{13}e^{i\delta} & c_{12}c_{23} - s_{12}s_{23}s_{13}e^{i\delta} & s_{23}c_{13} \\ s_{12}s_{23} - c_{12}c_{23}s_{13}e^{i\delta} & -c_{12}s_{23} - s_{12}c_{23}s_{13}e^{i\delta} & c_{23}c_{13} \end{bmatrix},
\tag{1}
$$

is used for the MNS matrix throughout this paper where c_{ij} and s_{ij} $(i,j = 1-3)$ imply $\cos\theta_{ij}$ and $\sin\theta_{ij}$, respectively. The mass squared difference of neutrinos is defined as $\Delta m_{ij}^2 \equiv m_i^2 - m_j^2$ where m_i is the mass of the ith eigenstate.

We examine possible "contamination" by δ, the matter effect, the sign of Δm_{31}^2, and the solar parameters one by one. We first note that, due to its low neutrino energy of a few MeV, the reactor experiments are inherently disappearance experiments, which can measure only the survival probability $P(\bar{\nu}_e \to \bar{\nu}_e)$. It is well known that the survival probability does not depend on the CP phase δ in arbitrary matter densities [28].

In any reactor experiment on the Earth, short or long baseline, the matter effect is very small because the energy is quite low and can be ignored to a good approximation. It can be seen by comparing the matter and the vacuum effects (as the matter correction comes in only through this combination in the approximate formula in [18])

$$
\frac{aL}{|\Delta_{31}|} = 2.8 \times 10^{-4} \left(\frac{|\Delta m_{31}^2|}{2.5 \times 10^{-3}\,\mathrm{eV}^2} \right)^{-1} \left(\frac{E}{4\,\mathrm{MeV}} \right) \left(\frac{\rho}{2.3\,\mathrm{g \cdot cm^{-3}}} \right) \left(\frac{Y_e}{0.5} \right),
\tag{2}
$$

where

$$
\Delta_{ij} \equiv \frac{\Delta m_{ij}^2 L}{2E}
\tag{3}
$$

with E being the neutrino energy and L baseline length. The best fit value of $|\Delta m_{31}^2|$ is given by $|\Delta m_{31}^2| = 2.5 \times 10^{-3}\,\mathrm{eV}^2$ from the Super-Kamiokande atmospheric neutrino data [29], and we use this as the reference value for $|\Delta m_{31}^2|$ throughout this paper. $a = \sqrt{2}G_F N_e$ denotes the index of refraction in matter with G_F being the Fermi constant and N_e the electron number density in the Earth which is related to the Earth matter density ρ as $N_e = Y_e\rho/m_p$ where Y_e is proton fraction. Once we know that the matter effect is negligible we immediately recognize that the survival probability is independent of the sign of Δm_{31}^2.

Therefore, the vacuum probability formula applies. The general probability formula in vacuum is analytically written as [27]

$$
\left\{ \begin{array}{l} P(\nu_\alpha \to \nu_\beta) \\ P(\bar{\nu}_\alpha \to \bar{\nu}_\beta) \end{array} \right\} = \delta_{\alpha\beta} - 4 \sum_{j<k} \mathrm{Re}\left(U_{\alpha j} U_{\beta j}^* U_{\alpha k}^* U_{\beta k} \right) \sin^2\left(\frac{\Delta m_{jk}^2 L}{4E} \right)
$$

$$
\mp 2 \sum_{j<k} \mathrm{Im}\left(U_{\alpha j} U_{\beta j}^* U_{\alpha k}^* U_{\beta k} \right) \sin\left(\frac{\Delta m_{jk}^2 L}{2E} \right),
\tag{4}
$$

3

where $\alpha, \beta = e, \mu, \tau$, and the minus and signs in front of the $\mathrm{Im}\left(U_{\alpha j}U_{\beta j}^* U_{\alpha k}^* U_{\beta k}\right)$ term in (4) correspond to neutrino and antineutrino channels, respectively. From (4) the exact expression for $P(\bar{\nu}_e \to \bar{\nu}_e)$ is given by

$$
\begin{aligned}
1 - P(\bar{\nu}_e \to \bar{\nu}_e) \;=\; & 4 \sum_{j<k} |U_{ej}|^2 |U_{ek}|^2 \sin^2\left(\frac{\Delta m_{jk}^2 L}{4E}\right) \\
=\; & \sin^2 2\theta_{13} \sin^2 \frac{\Delta_{31}}{2} + \frac{1}{2} c_{12}^2 \sin^2 2\theta_{13} \sin \Delta_{31} \sin \Delta_{21} \\
& + \left(c_{13}^4 \sin^2 2\theta_{12} + c_{12}^2 \sin^2 2\theta_{13} \cos \Delta_{31}\right) \sin^2 \frac{\Delta_{21}}{2},
\end{aligned} \tag{5}
$$

where the parametrization (1) has been used in the second line. The three terms in the second line of (5) are suppressed relative to the main depletion term, the first term of the right-hand-side of (5) , by ϵ, $\epsilon^2/\sin^2 2\theta_{13}$, ϵ^2, respectively, where $\epsilon \equiv \Delta m_{21}^2/|\Delta m_{31}^2|$. Assuming that $|\Delta m_{31}^2| = (1.6\text{-}3.9) \times 10^{-3}\,\mathrm{eV}^2$ [29], $\epsilon \simeq 0.1\text{-}0.01$ for the LMA MSW solar neutrino solution [3, 10]. Then, the first and the third terms in the second line can be ignored, although the second term can be of order unity compared with the main depletion term provided that $\epsilon \simeq 0.1$. (Notice that we are considering the measurement of $\sin^2 2\theta_{13}$ in the range of 0.1-0.01.) Therefore, assuming that $|\Delta m_{31}^2|$ is determined by LBL experiments with good accuracy, the reactor $\bar{\nu}_e$ disappearance experiment gives us a clean measurement of θ_{13} which is independent of any solar parameters except for the case of high Δm_{21}^2 LMA solutions.

If the high Δm_{21}^2 LMA solution with $\Delta m_{21}^2 \sim 10^{-4}\,\mathrm{eV}^2$ turns out to be the right one, we need a special care for the second term of the second line of (5). In this case, the determination of θ_{13} and the solar angle θ_{12} is inherently coupled,[1] and we would need joint analysis of near-far detector complex (see the next section) and KamLAND.

III. NEAR-FAR DETECTOR COMPLEX: BASIC CONCEPTS AND ESTIMATION OF SENSITIVITY

In order to obtain good sensitivity to $\sin^2 2\theta_{13}$, selection of an optimized baseline and having the small statistical and systematic errors are crucial. For instance, the baseline length that gives the oscillation maximum for reactor $\bar{\nu}_e$'s which have typical energy $4\,\mathrm{MeV}$ is $1.7\,\mathrm{km}$ for $\Delta m^2 \simeq 2.5 \times 10^{-3}\,\mathrm{eV}^2$. Along with this baseline selection, if systematic and statistical errors can be reduced to $1\,\%$ level, which is 2.8 times better than the CHOOZ experiment [6], an order of magnitude improvement for the $\sin^2 2\theta_{13}$ sensitivity is possible at $\Delta m^2 \simeq 2.5 \times 10^{-3}\,\mathrm{eV}^2$. In this section we demonstrate that such kind of experiment is potentially possible if we place a CHOOZ-like detector at a baseline $1.7\,\mathrm{km}$ in $200\,\mathrm{m}$ underground near a reactor of $24.3\,\mathrm{GW_{th}}$ thermal power. The reactor can be regarded as a simplified one of the Kashiwazaki-Kariwa nuclear power plant which consists of seven reactors and whose maximum energy generation is $24.3\,\mathrm{GW_{th}}$.

Major part of systematic errors is caused by uncertainties of the neutrino flux calculation, number of protons, and the detection efficiency. For instance, in the CHOOZ experiment, the uncertainty of the neutrino flux is $2.1\,\%$, that of number of protons is $0.8\,\%$, and that of

---

[1] The effect of nonzero θ_{13} for measurement of θ_{12} at KamLAND is discussed in [30].

detection efficiency 1.5 % as is shown in the Table I. The uncertainty of the neutrino flux includes ambiguities of the reactor thermal power generation, the reactor fuel component, the neutrino spectra from fissions, and so on. The uncertainty of the detection efficiency includes systematic shift of defining the fiducial volume. These systematic uncertainties, however, cancel out if identical detectors are placed near and far from the reactors and data taken at the detectors are compared.[2]

To estimate how good the cancellation will be, we study the case of the Bugey experiment, which uses three identical detectors to detect reactor neutrinos at 14/40/90 m. For the Bugey case, the uncertainty of the neutrino flux improved from 3.5 % to 1.7 % and the error on the solid angle remained the same (0.5 % → 0.5 %). If each ratio of the improvement for the Bugey case is directly applicable to our case, the systematic uncertainty will improve from 2.7 % to 0.8 % as shown in the Table I. The ambiguity of the solid angle will be negligibly small because the absolute baseline is much longer than the Bugey case. We are thinking of a case that a front detector is located at 300 m away from the reactor we consider. In the actual setting with the Kashiwazaki-Kariwa power plant two near detectors may be necessary due to extended array of seven reactors. Hereafter, we take 2 % and 0.8 % as the reference values of the relative systematic error $\sigma_{\rm sys}$ for the total number of $\bar{\nu}_e$ events in our analysis. Let us examine the physics potential of such a reactor experiment assuming these reference values for the systematic error. We take, for concreteness, the Kashiwazaki-Kariwa reactor of 24.3 GW$_{\rm th}$ thermal power and assume its operation with 80 % efficiency. Two identical liquid scintillation detectors are located at 300 m and 1.7 km away from the reactor and assumed to detect $\bar{\nu}_e$ by delayed coincidence with 70 % detection efficiency. The $\bar{\nu}_e$'s of 1-8 MeV visible energy, $E_{\rm visi} = E_{\bar{\nu}_e} - 0.8$ MeV, are used and the number of events are counted in 14 bins of 0.5 MeV. Without oscillation, a 10 (40) ton-year measurement at the far detector yields 20,000 (80,000) $\bar{\nu}_e$ events which is naively comparable to a 0.7 (0.35) % statistical error.

First, let us calculate how much we could constrain $\sin^2 2\theta_{13}$. Unlike the analysis in [31] which uses the ratio of the numbers of events at the near and the far detectors, we use the difference of the numbers of events $N_i(L_2) - (L_1/L_2)^2 N_i(L_1)$, because the statistical analysis with ratios is complicated. (See, e.g., [32].) The definition of $\Delta\chi^2$, which stands for the deviation from the best fit point (non-oscillation point) is given by

$$
\Delta\chi^2(\sin^2 2\theta_{13}, |\Delta m_{31}^2|)
$$
$$
\equiv \sum_{i=1}^{14} \frac{\left\{ \left[N_{i(0)}(L_2) - \left(\frac{L_1}{L_2}\right)^2 N_{i(0)}(L_1) \right] - \left[N_i(L_2) - \left(\frac{L_1}{L_2}\right)^2 N_i(L_1) \right] \right\}^2}{N_{i(0)}(L_2) + \left(\frac{L_1}{L_2}\right)^4 N_{i(0)}(L_1) + (\sigma_{\rm sys}^{\rm bin})^2 N_{i(0)}^2(L_2)}, \tag{6}
$$

$$
N_i(L_j) \equiv N_i(\sin^2 2\theta_{13}, |\Delta m_{31}^2|; L_j), \quad N_{i(0)}(L_j) \equiv N_i(0, 0; L_j),
$$

where $\sigma_{\rm sys}^{\rm bin}$ is the relative systematic error for each bin which is assumed to be the same for all bins and $N_i(\sin^2 2\theta_{13}, |\Delta m_{31}^2|)$ denotes the theoretical number of $\bar{\nu}_e$ events within the

---

[2] This is more or less the strategy taken in the Bugey experiment [31]. The Krasnoyarsk group also plans in their Kr2Det proposal [11] to construct two identical 50 ton liquid scintillators at 1100 m and 150 m away from the Krasnoyarsk reactor. They indicate that the systematic error can be reduced to 0.5 % by comparing the front and far detector.

ith energy bin. In principle both the systematic errors $\sigma_{\rm abs.sys}^{\rm bin}$ (absolute normalization) and $\sigma_{\rm sys}^{\rm bin}$ (relative normalization) appear in the denominator of (6), but by taking the difference, we have $(1 + \sigma_{\rm abs.sys}^{\rm bin})[(1 + \sigma_{\rm sys}^{\rm bin})N_i(L_2) - (L_1/L_2)^2 N_i(L_1)] - [N_i(L_2) - (L_1/L_2)^2 N_i(L_1)] = \sigma_{\rm sys}^{\rm bin} N_i(L_2) + \sigma_{\rm abs.sys}^{\rm bin}[N_i(L_2) - (L_1/L_2)^2 N_i(L_1)]$ which indicates that the systematic error is dominated by the relative error $\sigma_{\rm sys}^{\rm bin}$, as the second term $[N_i(L_2) - (L_1/L_2)^2 N_i(L_1)]$ is supposed to be small. In fact we have explicitly verified numerically that the presence of $(\sigma_{\rm abs.sys}^{\rm bin})^2 [N_i(L_2) - (L_1/L_2)^2 N_i(L_1)]^2$ in the denominator of (6) does not affect any result. From the assumption that the relative systematic error for each bin is distributed equally into bins, $\sigma_{\rm sys}^{\rm bin}$ is estimated from the relative systematic error $\sigma_{\rm sys}$ for the total number of events by

$$(\sigma_{\rm sys}^{\rm bin})^2 = \sigma_{\rm sys}^2 \frac{(N_{(0)}^{\rm tot}(L_2))^2}{\sum_i N_{i(0)}^2(L_2)}, \quad N_{(0)}^{\rm tot}(L_2) \equiv \sum_i N_{i(0)}(L_2), \tag{7}$$

since the uncertainty squared of the total number of events is obtained by adding up the bin-by-bin systematic errors $(\sigma_{\rm sys}^{\rm bin})^2 N_{i(0)}^2(L_2)$; The ratio $\sigma_{\rm sys}^{\rm bin}/\sigma_{\rm sys}$ is about 3 in our analysis. In Fig. 1, the 90 % CL exclusion limits, which corresponds to $\Delta\chi^2 = 2.7$ for 1 degree of freedom, are presented for two cases: a 10 ton-year measurement with the 2 % systematic error of the total number of events and a 40 ton-year measurement with the 0.8 % error. The figure shows that it is possible to measure $\sin^2 2\theta_{13}$ down to 0.02 at the maximum sensitivity with respect to $|\Delta m_{31}^2|$, and to 0.04 for larger $|\Delta m_{31}^2|$ by a 40 ton-year measurement, provided the quoted values of the systematic errors are realized. The CHOOZ result [6] is also depicted in Fig. 1. For a fair comparison with the CHOOZ contour, we also present in Fig. 1 the results of analysis with 2 degrees of freedom, which correspond to $\Delta\chi^2 = 4.6$ for 90 % CL, without assuming any precise knowledges on $|\Delta m_{31}^2|$.

Next, let us examine how precisely we could measure $\sin^2 2\theta_{13}$. The definition of $\Delta\chi^2$ is

$$\Delta\chi^2(\sin^2 2\theta_{13}, |\Delta m_{31}^2|)$$
$$\equiv \sum_{i=1}^{14} \frac{\left\{ \left[N_{i({\rm best})}(L_2) - \left(\frac{L_1}{L_2}\right)^2 N_{i({\rm best})}(L_1) \right] - \left[N_i(L_2) - \left(\frac{L_1}{L_2}\right)^2 N_i(L_1) \right] \right\}^2}{N_{i({\rm best})}(L_2) + \left(\frac{L_1}{L_2}\right)^4 N_{i({\rm best})}(L_1) + (\sigma_{\rm sys}^{\rm bin})^2 N_{i({\rm best})}^2(L_2)}, \tag{8}$$

where $N_{i({\rm best})}$ denotes N_i for the set of the best fit parameters $(\sin^2 2\theta_{13}^{({\rm best})}, |\Delta m_{31}^{2({\rm best})}|)$ given artificially. $\sigma_{\rm sys}^{\rm bin}$ is obtained in (7) by replacing $N_{i(0)}$ with $N_{i({\rm best})}$ and the ratio $\sigma_{\rm sys}^{\rm bin}/\sigma_{\rm sys}$ is about 3 again. We assume that the value of $|\Delta m_{31}^2|$ is known to a precision of $10^{-4}\,{\rm eV}^2$ by the JHF phase I by the time the reactor measurement is actually utilized to solve the degeneracy. Then, we rely on the analysis with 1 degree of freedom, fixing $|\Delta m_{31}^2|$ as $|\Delta m_{31}^{2({\rm best})}| = 2.5 \times 10^{-3}\,{\rm eV}^2$. The 90 % CL allowed regions of 1 degree of freedom, whose bounds correspond to $\Delta\chi^2 = 2.7$, are presented in Fig. 2 for the values of $\sin^2 2\theta_{13}^{({\rm best})}$ from 0.05 to 0.08 (0.02 to 0.08) in the unit of 0.01 in the case of a 10 ton-year (40 ton-year) measurement with systematic error $\sigma_{\rm sys} = 2.0(0.8)$ %. We can read off the errors at 90 % CL in $\sin^2 2\theta_{13}$ and it is almost independent of the central value $\sin^2 2\theta_{13}^{({\rm best})}$. Thus, we have

$$\sin^2 2\theta_{13} = \sin^2 2\theta_{13}^{({\rm best})} \pm 0.043 \quad (\text{at } 90\,\%\,{\rm CL, d.o.f.} = 1)$$
$$\text{for} \quad \sin^2 2\theta_{13}^{({\rm best})} \gtrsim 0.05$$

in the case of $\sigma_{\text{sys}} = 2\,\%$ with a 10 ton-year measurement, and

$$
\begin{aligned}
\sin^2 2\theta_{13} &= \sin^2 2\theta_{13}^{(\text{best})} \pm 0.018 \qquad (\text{at } 90\,\%\,\text{CL, d.o.f.} = 1)\\
& \text{for} \quad \sin^2 2\theta_{13}^{(\text{best})} \gtrsim 0.02
\end{aligned}
$$

in the case of $\sigma_{\text{sys}} = 0.8\,\%$ with a 40 ton-year measurement.

IV. THE PROBLEM OF THE (θ_{13}, δ, θ_{23}, Δm_{31}^2) PARAMETER DEGENERACY

We explore in this and the following sections the possible significance of reactor measurements of θ_{13} in the context of the problem of the parameter degeneracy. We show that the reactor measurement of θ_{13} can resolve the degeneracy at least partly if the measurement is sufficiently accurate. Toward the goal we first explain what is the problem of the parameter degeneracy in long-baseline neutrino oscillation experiments. It is a notorious problem; a set of measurements of the ν_μ disappearance probability and the appearance oscillation probabilities of $\nu_\mu \to \nu_e$ and $\bar{\nu}_\mu \to \bar{\nu}_e$, no matter how accurate they may be, does not allow unique determination of θ_{13}, δ, and θ_{23}. The problem was first recognized in the form of intrinsic degeneracy between the two sets of solutions of $(\theta_{23}, \theta_{13})$ for a given set of measurements in two different channels $\nu_\mu \to \nu_e$ and $\nu_\mu \to \nu_\tau$ [21]. It was then observed independently that the similar degeneracy of solutions of (θ_{13}, δ) exists in measurement of ν_e appearance in neutrino and antineutrino channels [22]. They made the first systematic analysis of the degeneracy problem. It was noticed that the degeneracy is further duplicated provided that the two neutrino mass patterns, the normal $(\Delta m_{31}^2 > 0)$ and the inverted $(\Delta m_{31}^2 < 0)$ hierarchies, are allowed [23]. Finally, it was pointed out that the degeneracy can be maximally eight-fold [24]. Analytic structure of the degenerate solutions was worked out in a general setting in [26].

To illuminate the point, let us first restrict our treatment to a relatively short baseline experiment such as the CERN-Frejus project [16]. In this case, one can use the vacuum oscillation approximation for the disappearance and the appearance probabilities. From the general formula (4) we have

$$
\begin{aligned}
1 - P(\nu_\mu \to \nu_\mu) &= 4 \sum_{j<k} |U_{\mu j}|^2 |U_{\mu k}|^2 \sin^2\left(\frac{\Delta m_{jk}^2 L}{4E}\right)\\
&= \sin^2 2\theta_{23} \sin^2 \frac{\Delta_{31}}{2}\\
& - \left(\frac{1}{2} c_{12}^2 \sin^2 2\theta_{23} - s_{13} s_{23}^2 \sin 2\theta_{23} \sin 2\theta_{12} \cos\delta\right) \sin\Delta_{21} \sin\Delta_{31}\\
& + O(\epsilon^2) + O(s_{13}^2),
\end{aligned}
\qquad (9)
$$

$$\left\{\begin{array}{c} P(\nu_\mu \to \nu_e) \\ P(\bar\nu_\mu \to \bar\nu_e) \end{array}\right\} = -4\sum_{j<k} \mathrm{Re}\left(U_{\mu j}U_{ej}^* U_{\mu k}^* U_{ek}\right)\sin^2\left(\frac{\Delta m_{jk}^2 L}{4E}\right)$$

$$\mp 2\sum_{j<k} \mathrm{Im}\left(U_{\mu j}U_{ej}^* U_{\mu k}^* U_{ek}\right)\sin\left(\frac{\Delta m_{jk}^2 L}{2E}\right),$$

$$= s_{23}^2 \sin^2 2\theta_{13}\sin^2\frac{\Delta_{31}}{2}$$

$$+ \frac{1}{2}J_r \sin\Delta_{21}\sin\Delta_{31}\cos\delta$$

$$\mp J_r\sin\Delta_{21}\sin^2\frac{\Delta_{31}}{2}\sin\delta + O(\epsilon s_{13}^2), \tag{10}$$

where $\epsilon \equiv \Delta m_{21}^2/|\Delta m_{31}^2|$, $J_r \equiv \sin 2\theta_{23}\sin 2\theta_{12}c_{13}^2 s_{13}$, and the parametrization (1) has been used in the second line in each formula. The minus and plus signs in front of $\sin\delta$ term in (10) correspond to neutrino and antineutrino channels, respectively. An explicit perturbative computation in [33] indicates that the matter effect enters into the expression in a particular combination with other quatities (in the form of $s_{13}^2 aL/\Delta_{31}$), so that the effect is small. By the disappearance measurement at JHF, for example, $\sin^2 2\theta_{23}$ and $|\Delta m_{31}^2|$ will be determined with accuracies of $1\,\%$ for $0.92 \leq \sin^2 2\theta_{23} \leq 1.0$ (Fig. 11 in [14]), and $4\,\%$ level, respectively [14].[3] If θ_{23} is not maximal, then we have two solutions for θ_{23} (θ_{23} and $\pi/2 - \theta_{23}$), even if we ignore the uncertainty in the determination of $\sin^2 2\theta_{23}$. For example, if $\sin^2 2\theta_{23} = 0.95$, which is perfectly allowed by the most recent atmospheric neutrino data [29], then s_{23}^2 can be either 0.39 or 0.61. Since the dominant term in the appearance probability depends upon s_{23}^2 instead of $\sin^2 2\theta_{23}$, it leads to $\pm 20\,\%$ difference in the number of appearance events in this case. On the other hand, in the case of maximal mixing, it still leaves a rather wide range of θ_{23}, despite such fantastic accuracy of the measurement. $1\,\%$ accuracy in $\sin^2 2\theta_{23}$ implies about $10\,\%$ uncertainty in s_{23}^2. Thus, whenever we try to determine $\sin^2 2\theta_{13}$ from the appearance measurement, we have to face the ambiguity due to the two-fold nature of the solution for s_{23}^2.

Let us discuss the simplest possible case, the LOW or the vacuum (VAC) oscillation solution of the solar neutrino problem. (See e.g., [34] for a recent discussion.) In this case, one can safely ignore terms of order ϵ in (9) and (10). Then we are left with only the first terms in the right-hand-side of these equations, the one-mass scale dominant vacuum oscillation probabilities. Now let us define the symbols $x = \sin^2 2\theta_{13}$ and $y = s_{23}^2$. Then, (9) and (10) take the forms $y = y_1$ or y_2 (corresponding to two solutions of s_{23}^2) and $xy = constant$, respectively, for given values of the probabilities. It is then obvious that there are two crossing points of these curves. This is the simplest version of the $(\theta_{13}, \theta_{23})$ degeneracy problem. We next discuss what happens if ϵ is not negligible though small: the case of LMA solar neutrino solution. In this case, the appearance curve, $xy = constant$, split into two curves (though they are in fact connected at their maximum value of s_{23}^2) because of the two degenerate solution of the set (δ, θ_{13}) that is allowed for a given set of values of s_{23}^2, $P(\nu_\mu \to \nu_e)$ and $P(\bar\nu_\mu \to \bar\nu_e)$. Then, we have, in general, four crossing points on the x–y plane for a given value of $\sin^2 2\theta_{23}$, the four-fold degeneracy. Simultaneously, the two $y = constant$

---

[3] Usually one thinks of determining not $|\Delta m_{31}^2|$ but $|\Delta m_{32}^2|$ by the disappearance measurement. But, it does not appear possible to resolve difference between these two quantities because one has to achieve resolution of order ϵ for the reconstructed neutrino energy.

lines are slightly tilted and the splitting between two curves becomes larger at larger $\sin^2 2\theta_{13}$, though the effect is too tiny to be clearly seen. If the baseline distance is longer, the Earth matter effect comes in and further splits each appearance contour into two, depending upon the sign of Δm_{31}^2. Then, we have four curves (or, two continuous contours each of which intersects with $y = constant$ line twice) and hence there are eight solutions as displayed in Fig. 3.[4] This is a simple pictorial representation of the maximal eight-fold parameter degeneracy [24]. To draw Fig. 3, we have calculated disappearance and appearance contours by using the approximate formula derived by Cervera *et al.* [18]. We take the baseline distance and neutrino energy as $L = 295\,\mathrm{km}$ and $E = 400\,\mathrm{MeV}$ with possible relevance to JHF project [14]. The Earth matter density is taken to be $\rho = 2.3\,\mathrm{g \cdot cm^{-3}}$ based on the estimate given in [35]. The electron fraction Y_e is taken to be 0.5. We assume, for definiteness, that a long-baseline disappearance measurement has resulted in $\sin^2 2\theta_{23} = 0.92$ and $\Delta m_{31}^2 = 2.5 \times 10^{-3}\,\mathrm{eV}^2$. For the LMA solar neutrino parameters we take $\tan^2 \theta_{12} = 0.38$ and $\Delta m_{21}^2 = 6.9 \times 10^{-5}\,\mathrm{eV}^2$ [36]. We take the values of these parameters and the matter density throughout this paper unless otherwise stated. The qualitative features of the figure remain unchanged even if we employ values of the parameters obtained by other analyses.

V. RESOLVING THE PARAMETER DEGENERACY BY REACTOR MEASUREMENT OF θ_{13}

Now we discuss how reactor experiments can contribute to resolve the parameter degeneracy. To make our discussion as concrete as possible we use the particular long-baseline experiment, the JHF experiment [14], to illuminate the complementary role played by reactor and long-baseline experiments. It is likely that the experiment will be carried out at around the first oscillation maximum ($|\Delta_{31}| = \pi$) for a number of reasons: the dip in energy spectrum in disappearance channel is the deepest, the number of appearance events are nearly maximal [14], and the two-fold degeneracy in δ becomes simple ($\delta \leftrightarrow \pi - \delta$) for each mass hierarchy [20, 24].[5] With the distance $L = 295\,\mathrm{km}$, the oscillation maximum is at around $E = 600\,\mathrm{MeV}$. We take the same mixing parameters as those used in Fig. 3.

A. Illustration of how reactor measurement helps resolve the (θ_{13}, θ_{23}) degeneracy

Let us first give an illustrative example showing how reactor experiments could help resolve the (θ_{13}, θ_{23}) degeneracy. To present a clear step-by-step explanation of the relationship between LBL and reactor experiments, we first plot in Fig. 4 the allowed regions in the $\sin^2 2\theta_{13}$–s_{23}^2 plane by measurements of $P(\nu_\mu \to \nu_e)$ alone and $P(\bar{\nu}_\mu \to \bar{\nu}_e)$ alone separately. The former is indicated by the regions bounded by black lines and the latter by gray lines. The solid and dashed lines are used for cases with positive and negative Δm_{31}^2. The values of disappearance and appearance probabilities are chosen arbitrarily for illustrative purpose

---

[4] The readers might be curious about the feature that the two contours are connected with each other at a large s_{23}^2 point. Because δ is a phase variable, the contours must be closed as δ varies.

[5] In order to have this reduction, one has to actually tune the energy spectrum so that $\cos \delta$ term in (10) averaged over the energy with the neutrino flux times the cross section vanishes, which is shown to be doable in [20].

and are given in the caption of Fig. 4. Notice that the negative Δm_{31}^2 curve is located right (left) to the positive Δm_{31}^2 curve in neutrino (antineutrino) channel. A plot with only measurement in neutrino mode goes beyond academic interest because the JHF experiment is expected to run only with the neutrino mode in its first phase. We observe that there is large intrinsic uncertainty in the θ_{13} determination due to unknown δ, the problem addressed in [20]. The two regions corresponding to positive and negative Δm_{31}^2 heavily overlap due to small matter effect. When two measurements of ν and $\bar{\nu}$ channels are combined, the allowed solution becomes a line which lies inside of the overlap of the ν and $\bar{\nu}$ regions for each sign of Δm_{31}^2 in Fig. 4. [6] In Fig. 5 we have plotted such solutions as two lines, one for positive Δm_{31}^2 (the solid curve) and the other for negative Δm_{31}^2 (the dashed curve) at the first oscillation maximum $|\Delta_{31}| = \pi$. It may appear curious that the two curves with positive and negative Δm_{31}^2 almost overlap with each other in Fig. 5. In fact, a slight splitting between the solid ($\Delta m_{31}^2 > 0$) and dashed ($\Delta m_{31}^2 < 0$) lines is due to the fact that both ϵ and the matter effect in the case of the JHF experiment are small. Thus, the degeneracy in the set (θ_{13}, θ_{23}) is effectively two-fold in this case.

To have a feeling on whether the reactor experiment described in Sec. III will be able to resolve the degeneracy, we plot in Fig. 5 two sets of degenerate solutions by taking a particular value of θ_{23}, $\sin^2 2\theta_{23} = 0.92$, the lower end of the region allowed by Super-Kamiokande. We denote the true and fake solutions as $(\sin^2 2\theta_{13}, s_{23}^2)$ and $(\sin^2 2\theta'_{13}, s_{23}^2{}')$, respectively, assuming the true θ_{23} satisfies $\theta_{23} < \pi/4$. We overlay in Fig. 5 a shadowed region to indicate the accuracy to be achieved by the reactor measurement of θ_{13}. If the experimental error $\delta_{\mathrm{re}}(\sin^2 2\theta_{13})$ in the reactor measurement of $\sin^2 2\theta_{13}$ is smaller than the difference

$$\delta_{\mathrm{de}}(\sin^2 2\theta_{13}) \equiv |\sin^2 2\theta'_{13} - \sin^2 2\theta_{13}| \tag{11}$$

due to the (θ_{13}, θ_{23}) degeneracy, then the reactor experiment may resolve the degeneracy. Notice that once the θ_{23} degeneracy is lifted one can easily obtain four allowed sets of (δ, Δm_{31}^2) (though they are still degenerate at almost the same point on the $\sin^2 2\theta_{13}$–s_{23}^2 plane) because the relationship between them is given analytically in a completely general setting [26].

B. Resolving power of the (θ_{13}, θ_{23}) degeneracy by a reactor measurement

Let us make a semi-quantitative estimate of how powerful the reactor method is for resolving the (θ_{13}, θ_{23}) degeneracy.[7] [8] For this purpose, we compare in this section the difference of the two θ_{13} solutions due to the degeneracy with the resolving power of the

---

[6] In the absence of the matter effect, the reason why the closed curve shrinks into a line at the the oscillation maximum can be seen as follows: By eliminating δ in (10), it is easy to show that there are two solutions of $\sin 2\theta_{13} > 0$ for given values of P, $\bar{P}$ and θ_{23} off the oscillation maximum ($\Delta_{31} \neq \pi$), whereas there is only one solution of $\sin 2\theta_{13} > 0$ at the oscillation maximum ($\Delta_{31} = \pi$). Even if we switch on the matter effect, one can easily show by using the approximate formula in [18] that the same argument holds.

[7] The possibility of resolving the (θ_{13}, θ_{23}) by a reactor experiment was qualitatively mentioned in [21, 34].

[8] An alternative way to resolve the ambiguity is to look at $\nu_e \rightarrow \nu_\tau$ channel because the main oscillation term in the probability $P(\nu_e \rightarrow \nu_\tau)$ depends upon c_{13}^2. Unfortunately, this idea does not appear to be explored in detail while it is briefly mentioned in [24, 25].

reactor experiment. We consider, for simplicity, the special case $|\Delta_{31}| = \pi$, i.e., energy tuned at the first oscillation maximum. The simplest case seems to be indicative of features of more generic cases.

As we saw in the previous section, there are two solutions of θ_{13} due to doubling of θ_{23} for a given $\sin^2 2\theta_{23}$ in each sign of Δm_{31}^2. Then, we define the fractional difference due to the degeneracy

$$\frac{\delta_{\mathrm{de}}(\sin^2 2\theta_{13})}{\sin^2 2\theta_{13}}. \tag{12}$$

It is to be compared with $\delta_{\mathrm{re}}(\sin^2 2\theta_{13})/\sin^2 2\theta_{13}$ of the reactor experiment, where $\delta_{\mathrm{re}}(\sin^2 2\theta_{13})$ denotes the experimental uncertainty estimated in Sec. III, i.e., 0.043 or 0.018. In Fig. 6(a) we plot the normalized error $\delta_{\mathrm{re}}(\sin^2 2\theta_{13})/\sin^2 2\theta_{13}$ which is expected to be achieved in the reactor experiment described in Sec. III. We restrict ourselves to the analysis with 1 degree of freedom, because we expect that the JHF phase I will provide us accurate information on Δm_{31}^2 by the time when the issue is really focused on the degeneracy in the JHF phase II. The fractional difference (12) can be computed from the relation [24]

$$\begin{aligned}
\sin^2 2\theta'_{13} &= \sin^2 2\theta_{13} \tan^2 \theta_{23} + \left(\frac{\Delta m_{21}^2}{\Delta m_{31}^2}\right)^2 \frac{\tan^2(aL/2)}{(aL/\pi)^2} \\
&\times \left[1 - (aL/\pi)^2\right] \sin^2 2\theta_{12} \left(1 - \tan^2 \theta_{23}\right),
\end{aligned} \tag{13}$$

and the result for $\delta_{\mathrm{de}}(\sin^2 2\theta_{13})/\sin^2 2\theta_{13}$ is plotted in Fig. 6(b) as a function of $\sin^2 \theta_{23}$ for two typical values of ϵ. We notice that the fractional differences differ by up to a factor of ~ 2 in small $\sin^2 2\theta_{23}$ region between the first ($\theta_{23} < \pi/4$) and the second octant ($\theta_{23} > \pi/4$). For the best fit value of the two mass squared differences Δm_{21}^2 ($6.9 \times 10^{-5}\,\mathrm{eV}^2$) and $|\Delta m_{31}^2|$ ($2.5 \times 10^{-3}\,\mathrm{eV}^2$), for which $\epsilon \equiv \Delta m_{21}^2/|\Delta m_{31}^2| = 0.028$, there is little difference between the case with $\sin^2 2\theta_{13} = 0.03$ and the one with $\sin^2 2\theta_{13} = 0.09$. In this case they are all approximated by the first term in (13) and $\delta_{\mathrm{de}}(\sin^2 2\theta_{13})/\sin^2 2\theta_{13}$ depends approximately only on θ_{23}, making the analysis easier. On the other hand, if the ratio $\epsilon \equiv \Delta m_{21}^2/|\Delta m_{31}^2|$ is much larger than that at the best fit point, then the second term in (13) is not negligible. In Fig. 6(b), $\delta_{\mathrm{de}}(\sin^2 2\theta_{13})/\sin^2 2\theta_{13}$ is plotted in an extreme case of $\epsilon = 1.9 \times 10^{-4}\,\mathrm{eV}^2/1.6 \times 10^{-3}\,\mathrm{eV}^2 = 0.12$, which is allowed at 90% CL (atmospheric) or 95% CL (solar), with $\sin^2 2\theta_{13} = 0.03, 0.06, 0.09$. From this, we observe that the suppression in the first term in (13) is compensated by the second term for $\sin^2 2\theta_{13} = 0.03$, i.e., the degeneracy is small and therefore resolving the degeneracy is difficult in this case. To clearly illustrate the resolving power of the degeneracy by the reactor measurement, assuming the best fit value $\epsilon = 0.028$, we plot in Fig. 7 the region where the degeneracy can be lifted in the $\sin^2 2\theta_{13}$–$\sin^2 2\theta_{23}$ plane. It is evident that the reactor measurement will be able to resolve the (θ_{13}, θ_{23}) degeneracy in a wide range inside its sensitivity region, in particular for θ_{23} in the second octant.

Quantitative estimation of the significance of the fake solution requires detailed analysis of accelerator experiments which includes the statistical and systematic errors as well as the correlations of errors and the parameter degeneracies, and it will be worked out in future communication.

VI. MORE ABOUT REACTOR VS. LONG-BASELINE EXPERIMENTS

The foregoing discussions in the previous section implicitly assume that the sensitivities of reactor and LBL experiments with both ν and $\bar{\nu}$ channels are good enough to detect effects of nonzero θ_{13}. However, it need not be true, in particular, in coming 10 years. To further illuminate complementary roles played by reactor and LBL experiments, we examine their possible mutual relationship including the cases where there is a signal in the former but none in the latter experiments, or vice versa. For ease of understanding by the readers, we restrict our presentation in this section to a very intuitive level by using a figure. It is, of course, possible to make it more precise by deriving inequalities based on the analytic approximate formulae [18]. Throughout this section LBL experiments at the oscillation maximum and $\theta_{23} = \pi/4$ are assumed.

If a reactor experiment sees an affirmative evidence for the disappearance in $\bar{\nu}_e \to \bar{\nu}_e$ (the case of Reactor Affirmative), it would be possible to determine θ_{13} up to certain experimental errors. In this case, the appearance probability in LBL experiment must fall into the region $P(\nu)_{\pm}^{\min} \leq P(\nu) \leq P(\nu)_{\pm}^{\max}$ if the mass hierarchy is known, where the $+(-)$ sign refers to $\Delta m_{31}^2 > 0$ ($\Delta m_{31}^2 < 0$) and max (min) refers to the maximum (minimum) value of the allowed region for $P \equiv P(\nu_\mu \to \nu_e)$, respectively. (See Fig. 8.) Without the knowledge of the mass hierarchy the probability is within the region $P(\nu)_{-}^{\min} \leq P(\nu) \leq P(\nu)_{+}^{\max}$. The similar inequalities are present also for antineutrino appearance channel. In Fig. 8 we present allowed regions in the cases of $\Delta m_{31}^2 > 0$ and $\Delta m_{31}^2 < 0$ on a plane spanned by $P(\nu_\mu \to \nu_e)$ and $P(\bar{\nu}_\mu \to \bar{\nu}_e)$ by taking two best fit values $\sin^2 2\theta_{13} = 0.08$, 0.04 (labeled as a, b) as reactor affirmative cases. They are inside the sensitivity region of the reactor experiment discussed in section III. We have used the one dimensional χ^2 analysis (i.e., the only parameter is $\sin^2 2\theta_{13}$) to obtain the allowed regions in Fig. 8. In doing this we have used the same systematic error of 0.8% and the statistical errors corresponding to 40 ton-year measurement by the detector considered in section III. For $\sin^2 2\theta_{13} \lesssim 0.02$, the particular reactor experiment would fail (the case of Reactor Negative) but the allowed region can be obtained by the same procedure, and presented in Fig. 8, the region labeled as c. We use the same LMA parameters as used earlier for Fig. 3 and Fig. 4.

We discuss four cases depending upon the two possibilities of affirmative and negative evidences (denoted as Affirmative, and Negative) in each disappearance and appearance search in reactor and long-baseline accelerator experiments, respectively. However, it is convenient to organize our discussion by classifying them into two categories, (Reactor Affirmative), and (Reactor Negative).

A. Reactor Affirmative

We have two alternative cases, the LBL appearance search Affirmative, or Negative.
LBL Affirmative:
Implications of affirmative evidence in the appearance search in LBL experiments differ depending upon which region the observed appearance probability $P(\nu)$ falls in:
(1) $P_{-}^{\min} \leq P(\nu) \leq P_{+}^{\min}$, or (2) $P_{-}^{\max} \leq P(\nu) \leq P_{+}^{\max}$:
These cases correspond to the two intervals which are given by the projection on the P axis of all the shadowed regions (a or b) minus the projection on the P axis of the darker shadowed region (a or b) in Fig. 8. It is remarkable that in these cases not only the sign of Δm_{31}^2 is determined, but also the CP phase δ is known to be nonvanishing. If $P(\nu)$ is in the

former region then Δm_{31}^2 is negative and $\sin \delta$ is positive, whereas if $P(\nu)$ is in the latter then Δm_{31}^2 is positive and $\sin \delta$ is negative.

(3) $P_+^{\min} \leq P(\nu) \leq P_-^{\max}$:

This case corresponds to the interval which is given by the projection on the P axis of the darker shadowed region (a or b) in Fig. 8. In this case, neither the sign of Δm_{31}^2 nor the sign of $\sin \delta$ can be determined.

It may be worth noting that if the reactor determination of θ_{13} is accurate enough, it could be advantageous for LBL appearance experiments to run only in the neutrino mode (where the cross section is larger than that for antineutrinos by a factor of 2-3) to possibly determine the sign of Δm_{31}^2 depending upon which region $P(\nu)$ falls in.

LBL Negative:

In principle, it is possible to have no appearance event even though the reactor sees evidence for disappearance. This case corresponds to the left edge of the analogous shadowed region in the case of $\sin^2 2\theta_{13} \simeq 0.02$ in Fig. 8, i.e., the allowed region with $\sin^2 2\theta_{13} \simeq 0.02$ for which $P_-^{\min}$ on the P axis falls below $P = 0.005$. In order for this case to occur the sensitivity limits $P(\nu)_{\text{limit}}$ of the LBL experiment must satisfy $P_-^{\min} < P(\nu)_{\text{limit}}$ assuming our ignorance to the sign of Δm_{31}^2. If it occurs that $P_-^{\min} < P(\nu)_{\text{limit}} < P_+^{\min}$, then the sign of Δm_{31}^2 is determined to be minus.

$P(\nu)_{\text{limit}}$ of the JHF experiment in its phase I is estimated to be 3×10^{-3} [14].[9] Therefore, by using the mixing parameters typical to the LMA solution, the case of LBL Negative cannot occur unless the sensitivity of the reactor experiment becomes $\sin^2 2\theta_{13} \lesssim 0.01$. However, in the intermediate stage of the JHF experiment, where $P(\nu)_{\text{limit}}$ is larger than 3×10^{-3}, this situation may occur.

B. Reactor Negative

If the reactor experiment does not see disappearance of $\bar{\nu}_e$ one obtains the bound $\theta_{13} \leq \theta_{13}^{\text{RL}}$. We have again two alternative cases, the LBL appearance search Affirmative, or Negative.

LBL Affirmative:

If a LBL experiment measures the oscillation probability $P(\nu)$. Then, for a given value of $P(\nu)$ the allowed region of $\sin 2\theta_{13}$ is given by $\sin 2\theta_\pm^{\min} \leq \sin 2\theta_{13} \leq \sin 2\theta_\pm^{\max}$ if the sign of Δm_{31}^2 is known, and by $\sin 2\theta_+^{\min} \leq \sin 2\theta_{13} \leq \sin 2\theta_-^{\max}$ otherwise. We denote below the maximum and the minimum values of θ_{13} collectively as $\theta_{\max}$ and $\theta_{\min}$, respectively. In Fig. 4, the region bounded by $\sin 2\theta_+^{\min}$ and $\sin 2\theta_+^{\max}$ ($\sin 2\theta_-^{\min}$ and $\sin 2\theta_-^{\max}$) are indicated as a region bounded by the solid (dashed) black line for a given value of s_{23}^2.

Then, there are two possibilities which we discuss one by one:

(i) $\theta_{13}^{\text{RL}} \geq \theta_{\max}$: In this case no additional information is obtained by nonobservation of disappearance of $\bar{\nu}_e$ in reactor experiment.

(ii) $\theta_{\min} \leq \theta_{13}^{\text{RL}} \leq \theta_{\max}$: In this case we have a nontrivial constraint $\theta_{\min} \leq \theta_{13} \leq \theta_{13}^{\text{RL}}$.

LBL Negative:

In this case, we obtain the upper bound on θ_{13}, which however depends on the assumed values of δ and the sign of Δm_{31}^2. A δ-independent bound can also be derived: $\theta_{13} \leq$

---

[9] The sensitivity limit of $\sin^2 2\theta_{13}$ quoted in [14], $\sin^2 2\theta_{13} \leq 6 \times 10^{-3}$, obtained by using one-mass scale approximation ($\epsilon \ll 1$) may be translated into this limit for $P(\nu)$.

$\min[\theta^{\mathrm{RL}}, \theta_{\max}]$.

VII. DISCUSSION AND CONCLUSION

In this paper, we have explored in detail the possibility of measuring $\sin^2 2\theta_{13}$ using reactor neutrinos. We stressed that this measurement is free from the problem of parameter degeneracies from which accelerator appearance experiments suffer, and that the reactor measurement is complementary to accelerator experiments. We have shown that the sensitivity to $\sin^2 2\theta_{13} \gtrsim 0.02$ (0.05) is obtained with a $24.3\,\mathrm{GW_{th}}$ reactor with identical detectors at near and far distances and with data size of 40 (10) ton-year assuming that the relative systematic error is 0.8% (2%) for the total number of events. In particular, if the relative systematic error is 0.8%, the error in $\sin^2 2\theta_{13}$ is 0.018 which is smaller than the uncertainty due to the combined (intrinsic and hierarchical) parameter degeneracies expected in accelerator experiments. We also have shown that the reactor measurement can resolve the degeneracy in $\theta_{23} \leftrightarrow \pi/2 - \theta_{23}$ and determine whether θ_{23} is smaller or larger than $\pi/4$ if $\sin^2 2\theta_{13}$ and $\cos^2 2\theta_{23}$ are relatively large.

We have taken 2% and 0.8% as the reference values for the relative systematic error for the total number of events. 2% is exactly the same figure as the Bugey experiment while 0.8% is what we naively expect in the case we have two identical detectors, near and far, which are similar to that of the CHOOZ experiment. It is also technically possible to dig a 200 m depth shaft hole with diameter wide enough to place a CHOOZ-like detector in. Therefore, the discussions in this paper are realistic. We hope the present paper stimulates interest of the community in reactor measurements of θ_{13}.

[1] Y. Fukuda *et al.* [Kamiokande Collaboration], Phys. Lett. B **335**, 237 (1994); Y. Fukuda *et al.* [Super-Kamiokande Collaboration], Phys. Rev. Lett. **81**, 1562 (1998) [arXiv:hep-ex/9807003]; S. Fukuda *et al.* [Super-Kamiokande Collaboration], Phys. Rev. Lett. **85**, 3999 (2000) [arXiv:hep-ex/0009001].

[2] B. T. Cleveland *et al.*, Astrophys. J. **496**, 505 (1998); J. N. Abdurashitov *et al.* [SAGE Collaboration], Phys. Rev. C **60**, 055801 (1999) [arXiv:astro-ph/9907113]; W. Hampel *et al.* [GALLEX Collaboration], Phys. Lett. B **447**, 127 (1999); S. Fukuda *et al.* [Super-Kamiokande Collaboration], Phys. Rev. Lett. **86**, 5651 (2001) [arXiv:hep-ex/0103032]; S. Fukuda *et al.* [Super-Kamiokande Collaboration], Phys. Rev. Lett. **86**, 5656 (2001) [arXiv:hep-ex/0103033]; Q. R. Ahmad *et al.* [SNO Collaboration], Phys. Rev. Lett. **87**, 071301

(2001) [arXiv:nucl-ex/0106015]; Q. R. Ahmad *et al.* [SNO Collaboration], Phys. Rev. Lett. **89**, 011301 (2002) [arXiv:nucl-ex/0204008].

[3] Q. R. Ahmad *et al.* [SNO Collaboration], Phys. Rev. Lett. **89**, 011302 (2002) [arXiv:nucl-ex/0204009].

[4] S. H. Ahn *et al.* [K2K Collaboration], Phys. Lett. B **511**, 178 (2001) [arXiv:hep-ex/0103001]; T. Nakaya [SUPER-KAMIOKANDE and K2K Collaborations], arXiv:hep-ex/0209036; K. Nishikawa, Nucl. Phys. Proc. Suppl. **118**, 129 (2003).

[5] Z. Maki, M. Nakagawa and S. Sakata, Prog. Theor. Phys. **28**, 870 (1962).

[6] M. Apollonio *et al.* [CHOOZ Collaboration], Phys. Lett. B **420**, 397 (1998) [arXiv:hep-ex/9711002]; M. Apollonio *et al.* [CHOOZ Collaboration], Phys. Lett. B **466**, 415 (1999) [arXiv:hep-ex/9907037].

[7] J. Shirai, Nucl. Phys. Proc. Suppl. **118**, 15 (2003).

[8] L. Wolfenstein, Phys. Rev. D **17**, 2369 (1978).

[9] S. P. Mikheyev and A. Yu. Smirnov, Yad. Fiz. **42**, 1441 (1985) [Sov. J. Nucl. Phys. **42**, 913 (1985)]; S. P. Mikheev and A. Y. Smirnov, Nuovo Cim. C **9**, 17 (1986).

[10] M. B. Smy, in *Neutrino Oscillations and Their Origin (Kashiwa 2001)*, edited by Y. Suzuki *et al.* (World Scientific, Singapre, 2003), p. 40 [arXiv:hep-ex/0202020]; J. N. Bahcall, M. C. Gonzalez-Garcia and C. Pena-Garay, JHEP **0207**, 054 (2002) [arXiv:hep-ph/0204314]; V. Barger, D. Marfatia, K. Whisnant and B. P. Wood, Phys. Lett. B **537**, 179 (2002) [arXiv:hep-ph/0204253]; A. Bandyopadhyay, S. Choubey, S. Goswami and D. P. Roy, Phys. Lett. B **540**, 14 (2002) [arXiv:hep-ph/0204286]; P. C. de Holanda and A. Y. Smirnov, Phys. Rev. D **66**, 113005 (2002) [arXiv:hep-ph/0205241]; G. L. Fogli, E. Lisi, A. Marrone, D. Montanino and A. Palazzo, Phys. Rev. D **66**, 053010 (2002) [arXiv:hep-ph/0206162]; M. Maltoni, T. Schwetz, M. A. Tortola and J. W. Valle, Phys. Rev. D **67**, 013011 (2003) [arXiv:hep-ph/0207227].

[11] Y. Kozlov, L. Mikaelyan and V. Sinev, arXiv:hep-ph/0109277.

[12] The MINOS Collaboration, P. Adamson *et al.*, *MINOS Detectors Technical Design Report, Version 1.0*, NuMI-L-337, October 1998
[http://www.hep.anl.gov/ndk/hypertext/minos_tdr.html].

[13] M. Komatsu, P. Migliozzi, and F. Terranova, J. Phys. G **29**, 443 (2003) [hep-ph/0210043].

[14] Y. Itow *et al.*, arXiv:hep-ex/0106019.

[15] H. Minakata and H. Nunokawa, Phys. Lett. B **495**, 369 (2000) [arXiv:hep-ph/0004114]; Nucl. Instrum. Meth. A **472**, 421 (2000) [arXiv:hep-ph/0009091]; J. Sato, Nucl. Instrum. Meth. A **472**, 434 (2000) [arXiv:hep-ph/0008056]; B. Richter, arXiv:hep-ph/0008222.

[16] J. J. Gomez-Cadenas *et al.* [CERN working group on Super Beams Collaboration], arXiv:hep-ph/0105297.

[17] D. Ayres *et al.* arXiv:hep-ex/0210005.

[18] A. Cervera, A. Donini, M. B. Gavela, J. J. Gomez Cadenas, P. Hernandez, O. Mena and S. Rigolin, Nucl. Phys. B **579**, 17 (2000) [Erratum-ibid. B **593**, 731 (2001)] [arXiv:hep-ph/0002108].

[19] C. Albright *et al.*, arXiv:hep-ex/0008064; V. D. Barger, S. Geer, R. Raja and K. Whisnant, Phys. Rev. D **63**, 113011 (2001) [arXiv:hep-ph/0012017]; J. Pinney and O. Yasuda, Phys. Rev. D **64**, 093008 (2001) [arXiv:hep-ph/0105087]; P. Hernandez and O. Yasuda, Nucl. Instrum. Meth. A **485**, 811 (2002); O. Yasuda, Nucl. Instrum. Meth. A **503**, 104 (2003); [arXiv:hep-ph/0111172]; in *Neutrino Oscillations and Their Origin (Kashiwa 2001)*, edited by Y. Suzuki *et al.* (World Scientific, Singapre, 2003), p. 259 [arXiv:hep-ph/0203273]; arXiv:hep-ph/0209127, and the references therein.

[20] T. Kajita, H. Minakata and H. Nunokawa, Phys. Lett. B **528**, 245 (2002) [arXiv:hep-ph/0112345].

[21] G. Fogli and E. Lisi, Phys. Rev. **D54**, 3667 (1996) [arXiv:hep-ph/9604415].

[22] J. Burguet-Castell, M. B. Gavela, J. J. Gomez-Cadenas, P. Hernandez and O. Mena, Nucl. Phys. B **608**, 301 (2001) [arXiv:hep-ph/0103258].

[23] H. Minakata and H. Nunokawa, JHEP **0110**, 001 (2001) [arXiv:hep-ph/0108085]; Nucl. Phys. Proc. Suppl. **110**, 404 (2002) [arXiv:hep-ph/0111131].

[24] V. Barger, D. Marfatia and K. Whisnant, Phys. Rev. D **65**, 073023 (2002) [arXiv:hep-ph/0112119]; in *Proc. of the APS/DPF/DPB Summer Study on the Future of Particle Physics (Snowmass 2001)* ed. R. Davidson and C. Quigg, arXiv:hep-ph/0108090.

[25] A. Donini, D. Meloni and P. Migliozzi, Nucl. Phys. B **646**, 321 (2002) [arXiv:hep-ph/0206034].

[26] H. Minakata, H. Nunokawa and S. Parke, Phys. Rev. D **66**, 093012 (2002) [arXiv:hep-ph/0208163].

[27] K. Hagiwara *et al.* [Particle Data Group Collaboration], Phys. Rev. D **66**, 010001 (2002).

[28] T. K. Kuo and J. Pantaleone, Phys. Lett. B **198**, 406 (1987); H. Minakata and S. Watanabe, Phys. Lett. B **468**, 256 (1999) [arXiv:hep-ph/9906530]. In a recent paper, the similar treatment is generalized into all other channels; H. Yokomakura, K. Kimura and A. Takamura, Phys. Lett. B **544**, 286 (2002) [arXiv:hep-ph/0207174].

[29] M. Shiozawa, Talk presented at XXth International Conference on Neutrino Physics and Astrophysics (Neutrino 2002), May 25-30, 2002, Munich, Germany.

[30] M. C. Gonzalez-Garcia and C. Pena-Garay, Phys. Lett. B **527**, 199 (2002) [arXiv:hep-ph/0111432].

[31] Y. Declais *et al.*, Nucl. Phys. B **434**, 503 (1995).

[32] G. L. Fogli and E. Lisi, Phys. Rev. D **52**, 2775 (1995) [arXiv:hep-ph/9504287].

[33] J. Arafune, M. Koike and J. Sato, Phys. Rev. **D56**, 3093 (1997) [arXiv:hep-ph/9703351], [Erratum *ibid.* **D 60**, 119905 (1999)].

[34] G. Barenboim and A. de Gouvea, arXiv:hep-ph/0209117.

[35] M. Koike and J. Sato, Mod. Phys. Lett. **A14**, 1297 (1999) [arXiv:hep-ph/9803212].

[36] S. Fukuda *et al.* [Super-Kamiokande Collaboration], Phys. Lett. B **539**, 179 (2002) [arXiv:hep-ex/0205075].

Bugey	absolute normalization	relative normalization	relative/absolute
flux	2.8%	0.0%	0
number of protons	1.9%	0.6%	0.32
solid angle	0.5%	0.5%	1
detection efficiency	3.5%	1.7%	0.49
total	4.9%	2.0%	

CHOOZ–like	absolute normalization	relative normalization (expected)	relative/absolute
flux	2.1%	0.0%	0
number of protons	0.8%	0.3%	0.38
detection efficiency	1.5%	0.7%	0.47
total	2.7%	0.8%	
for bins	8.1%	2.4%	

TABLE I: Systematic errors in the Bugey and the CHOOZ-like experiments. Relative errors in the CHOOZ-like experiment are expectation with the same reduction rates of errors as those of Bugey.
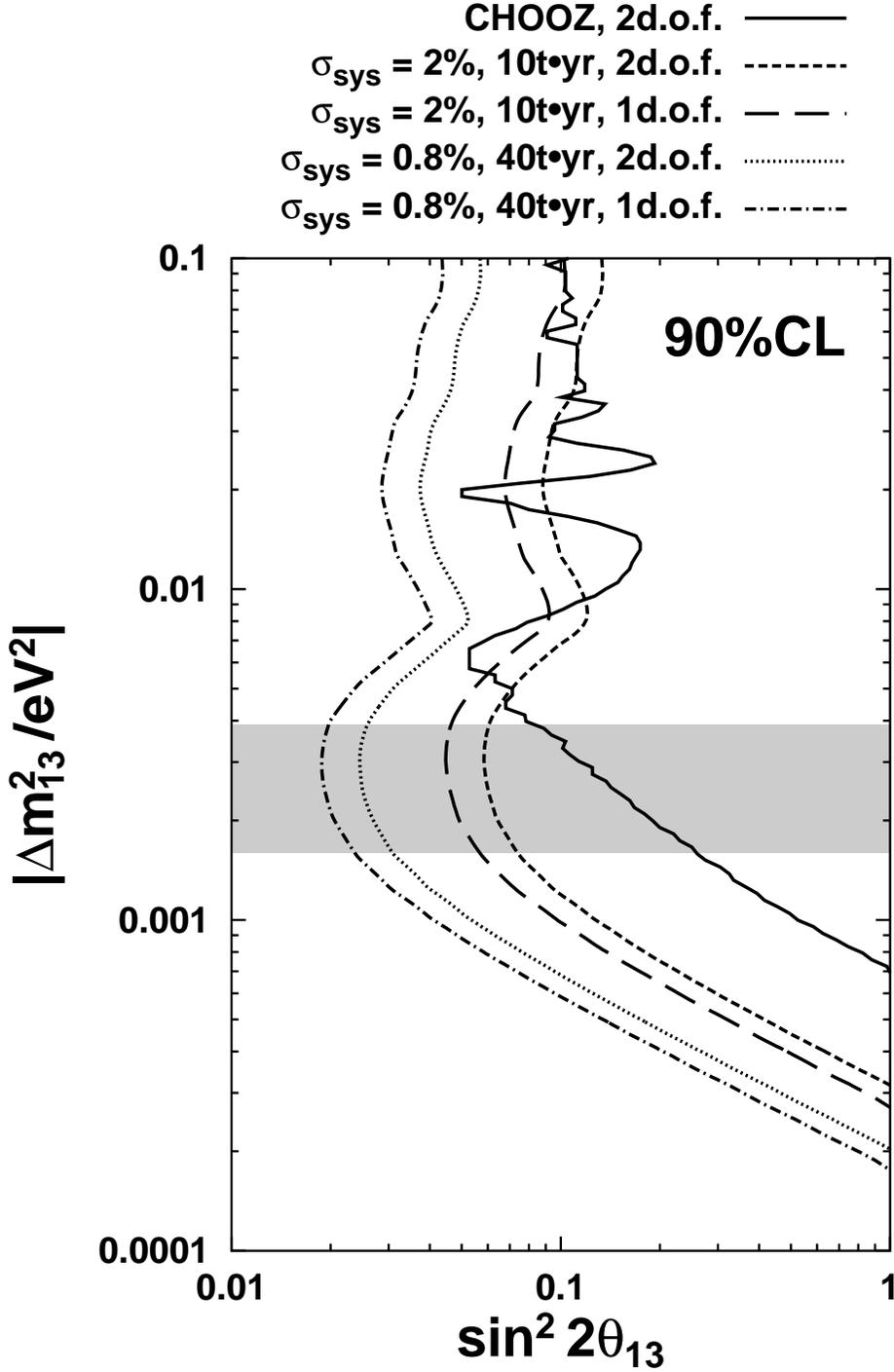
FIG. 1: Shown are the 90% CL exclusion limits on $\sin^2 2\theta_{13}$ which can be placed by the reactor measurement as described in Sec. III. From the left to right, the dash-dotted and the thin-dotted (the long-dashed and short-dashed) lines are based on analyses with 1 and 2 degrees of freedom (see the text), respectively for $\sigma_{\rm sys}$=0.8 %, 40 t·yr ($\sigma_{\rm sys}$=2 %, 10 t·yr). The solid line is the CHOOZ result, and the 90 % CL interval $1.6 \times 10^{-3}\,{\rm eV^2} \leq \Delta m_{31}^2 \leq 3.9 \times 10^{-3}\,{\rm eV^2}$ of the Super-Kamiokande atmospheric neutrino data is shown as a shaded strip.
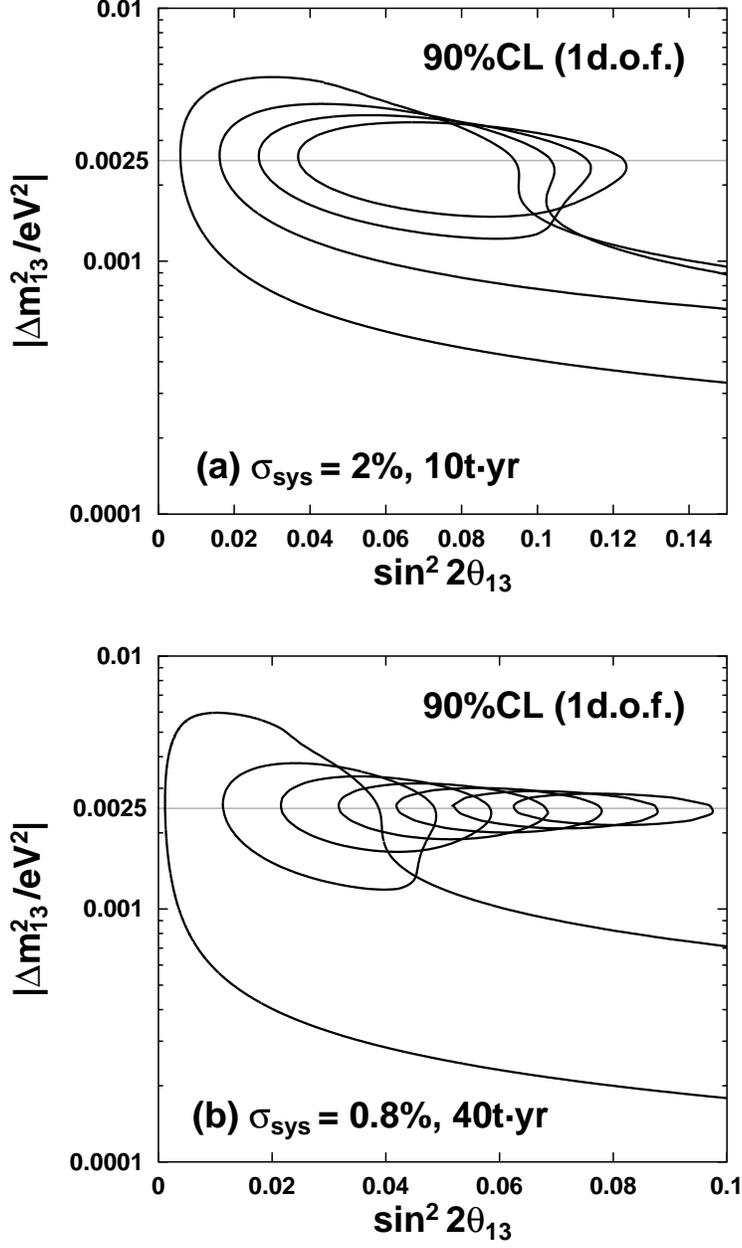
FIG. 2: Shown is the accuracy of determination of $\sin^2 2\theta_{13}$ at $90\,\%$ CL for the case of positive evidence based on analysis with 1 degree of freedom, $\Delta\chi^2 = 2.7$. Figures (a) and (b) are for $\sigma_{\rm sys}$=2%, 10 t·yr, and $\sigma_{\rm sys}$=0.8%, 40 t·yr, respectively. The lines correspond to the best fit values of $\sin^2 2\theta_{13}$, from left to right, 0.05 to 0.08 in the unit of 0.01 in Fig. 2(a), and 0.02 to 0.08 in the unit of 0.01 in Fig. 2(b). The reference value of $|\Delta m_{31}^{2({\rm best})}|$ is taken to be $2.5 \times 10^{-3}\,{\rm eV}^2$, which is indicated by a gray line.
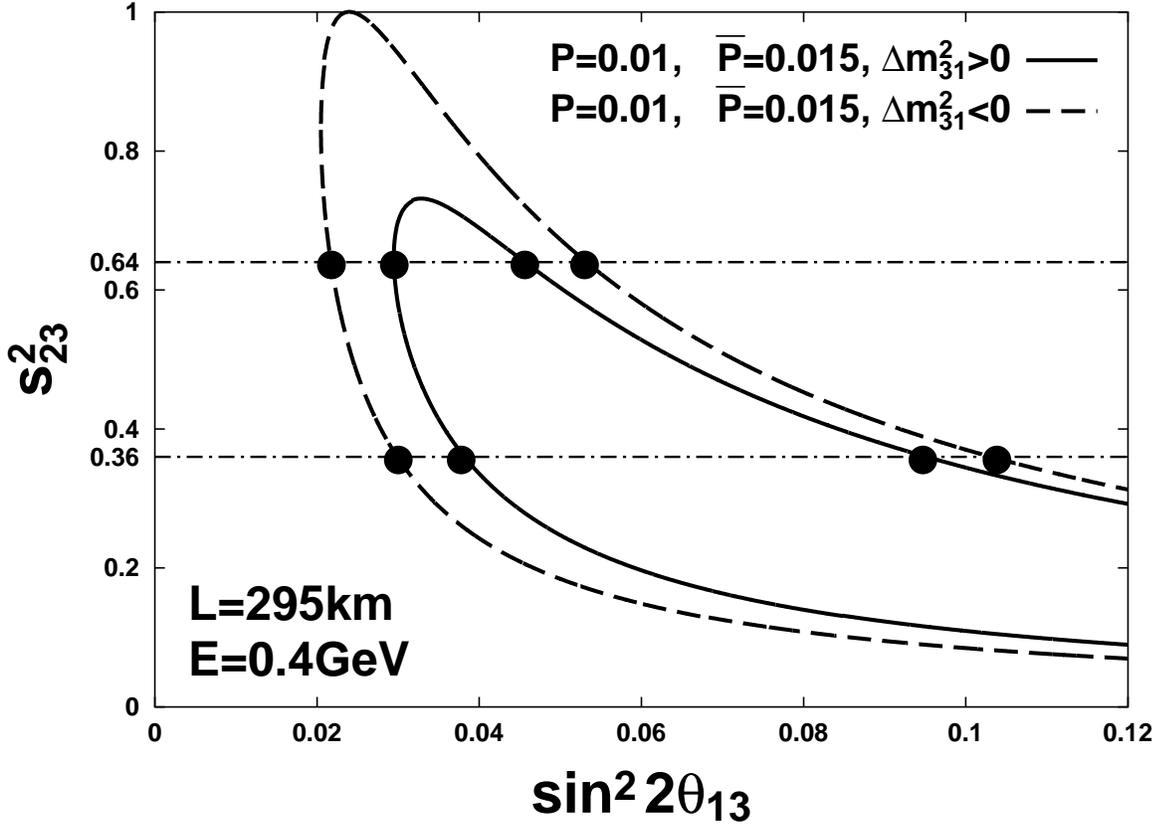
FIG. 3: Depicted in the $\sin^2 2\theta_{13}$–s_{23}^2 plane are the contours determined by arbitrarily given values of the appearance probabilities $P \equiv P(\nu_\mu \to \nu_e) = 0.01$ and $\bar{P} \equiv P(\bar{\nu}_\mu \to \bar{\nu}_e) = 0.015$ with E/L off the oscillation maximum ($|\Delta_{31}| \neq \pi$) at the JHF experiment. Here, $s_{23}^2 \equiv \sin^2 \theta_{23}$. The solid and the dashed lines correspond to positive and negative Δm_{31}^2, respectively. The dash-dotted lines represent the boundary of the region $0.36 \leq s_{23}^2 \leq 0.64$ which is presently allowed by the atmospheric neutrino data, $0.92 \leq \sin^2 2\theta_{23} \leq 1$. As indicated in the figure, there are four solutions for each s_{23}^2, and altogether there are eight solutions as denoted by blobs for any values of $\theta_{23} \neq \pi/4$. The oscillation parameters are taken as follows: $\Delta m_{31}^2 = 2.5 \times 10^{-3} \text{eV}^2$, $\Delta m_{21}^2 = 6.9 \times 10^{-5} \text{eV}^2$, $\tan^2 \theta_{12} = 0.38$. The Earth density is taken to be $\rho = 2.3$ g/cm^3.
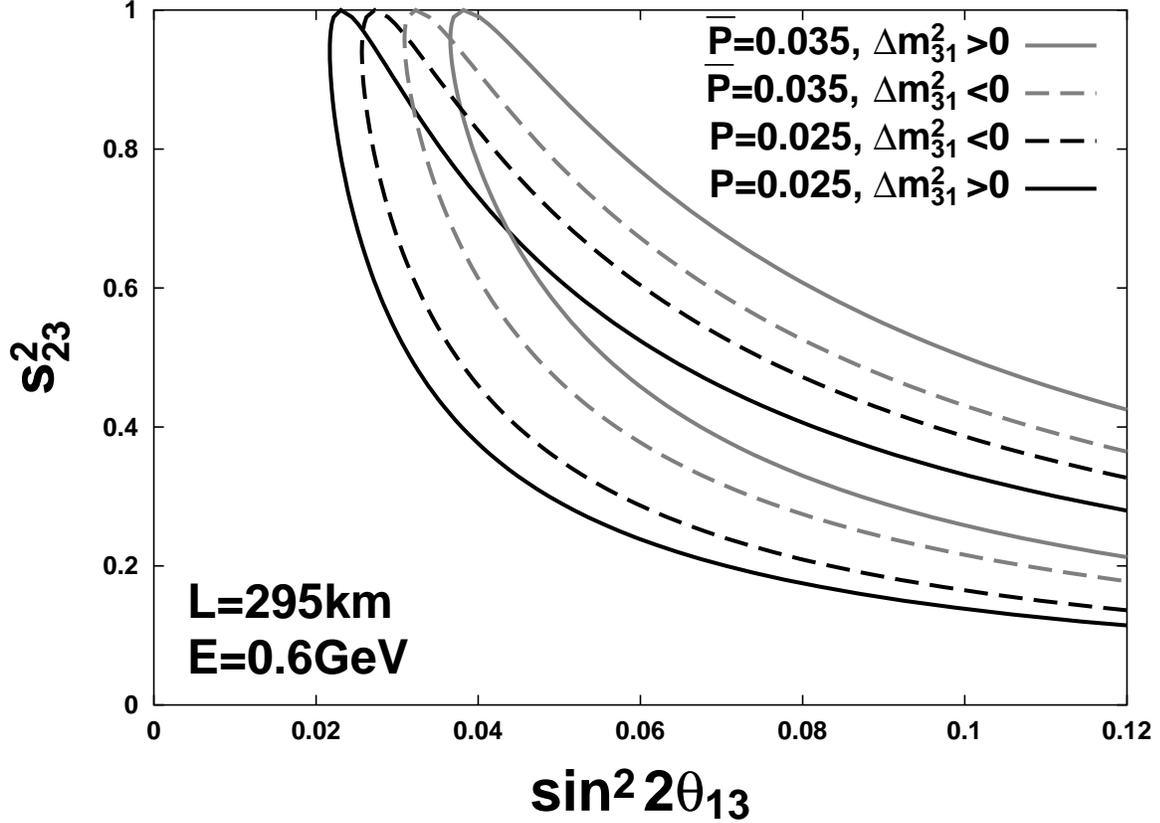
FIG. 4: The allowed regions are shown in the $\sin^2 2\theta_{13}$–s_{23}^2 plane determined with a given value of $P \equiv P(\nu_\mu \to \nu_e)$ alone (in this case $P = 0.025$), or $\bar{P} \equiv P(\bar{\nu}_\mu \to \bar{\nu}_e)$ alone (in this case $\bar{P} = 0.035$) at the oscillation maximum $|\Delta_{31}| = \pi$ of the JHF experiment. Each allowed region is the area bounded by the black solid (for $\Delta m_{31}^2 > 0$ with P only), the black dashed (for $\Delta m_{31}^2 < 0$ with P only), the gray solid (for $\Delta m_{31}^2 > 0$ with $\bar{P}$ only), the gray dashed (for $\Delta m_{31}^2 < 0$ with $\bar{P}$ only), respectively, where the line with a definite value of the CP phase δ sweeps out each region as δ varies from 0 to 2π. The oscillation parameters and the Earth density are the same as those in Fig. 3.
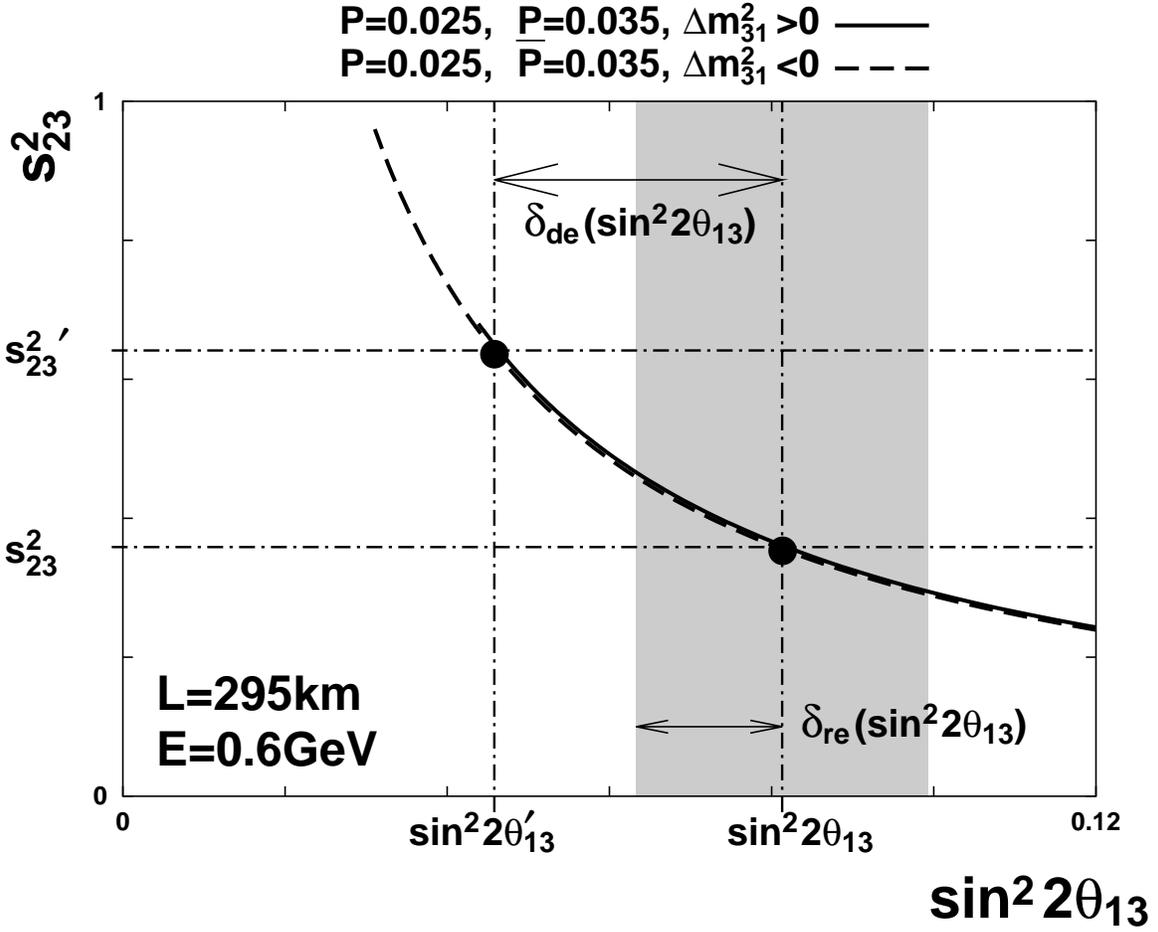
FIG. 5: The allowed region in the $\sin^2 2\theta_{13}$–s^2_{23} plane becomes a line when both $P(\nu_\mu \to \nu_e)$ and $P(\bar{\nu}_\mu \to \bar{\nu}_e)$ are given (in this case $P(\nu_\mu \to \nu_e) = 0.025$, $P(\bar{\nu}_\mu \to \bar{\nu}_e) = 0.035$) at the oscillation maximum ($|\Delta_{31}| = \pi$, $E = 0.6$ GeV for the JHF experiment), as indicated in the figure. The solid and the dashed lines are for $\Delta m^2_{31} > 0$ and $\Delta m^2_{31} < 0$ cases, respectively. Assuming $\theta_{23} \neq \pi/4$, two solutions of $(\sin^2 2\theta_{13}, s^2_{23})$ are plotted; In this figure $\sin^2 2\theta_{23}$ is taken as 0.92. It is assumed arbitrarily that the solution of θ_{23} in the first octant ($\theta_{23} < \pi/4$) is the genuine one, while the one in the second octant ($\theta_{23} > \pi/4$) with primes is the fake one. Superimposed in the figure as a shaded region is the anticipated error in the reactor measurement of θ_{13} estimated in Sec. III. If the error $\delta_{\mathrm{re}}(\sin^2 2\theta_{13})$ is smaller than the difference $\delta_{\mathrm{de}}(\sin^2 2\theta_{13}) \equiv |\sin^2 2\theta'_{13} - \sin^2 2\theta_{13}|$ due to the degeneracy, then the reactor experiment may be able to resolve it.
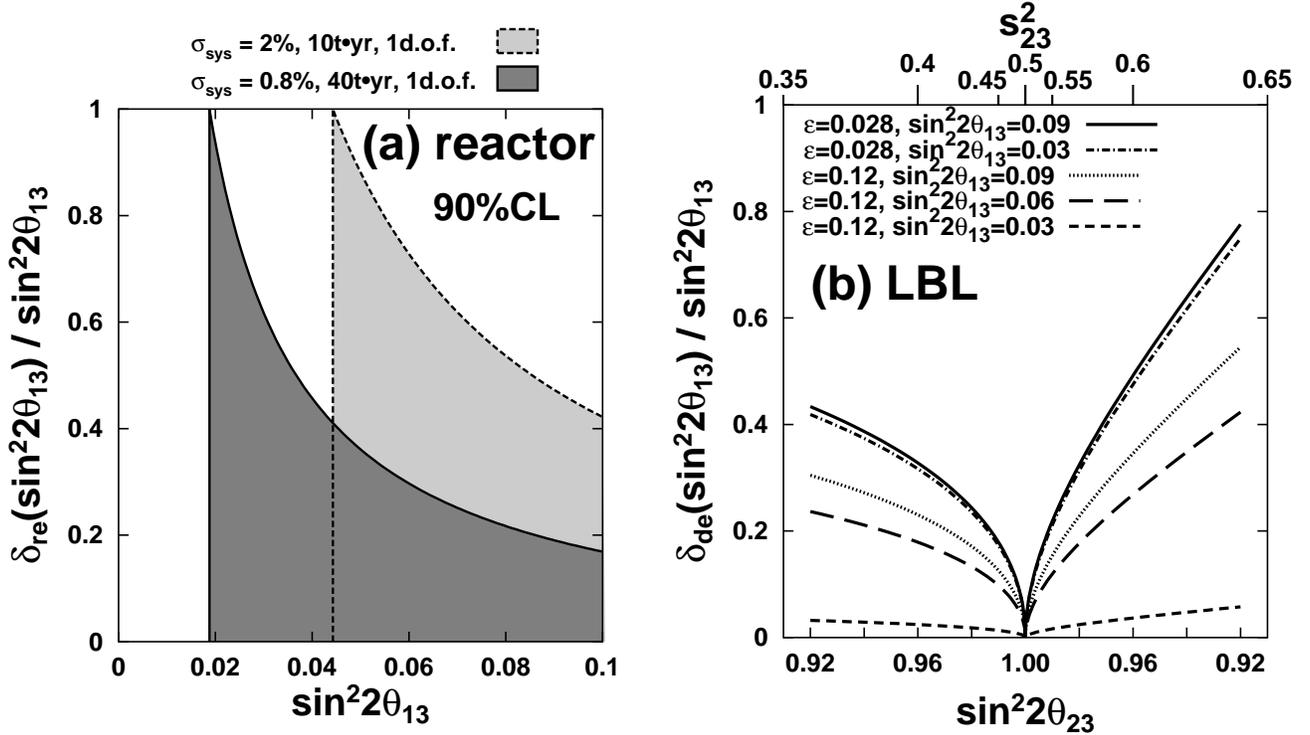
FIG. 6: (a) The normalized error at $90\,\%\,$CL in the reactor measurement of θ_{13} is given for $\sigma_{\text{sys}}{=}2\,\%$, $10\,$t·yr (d.o.f.=1, $\delta_{\text{re}}(\sin^2 2\theta_{13}) = 0.043$) and for $\sigma_{\text{sys}}{=}0.8\,\%$, $40\,$t·yr (d.o.f.=1, $\delta_{\text{re}}(\sin^2 2\theta_{13}) = 0.018$), respectively. Notice that the degrees of freedom becomes 1 once the value of $|\Delta m_{31}^2|$ is known from JHF.

(b) The fractional difference $\delta_{\text{de}}(\sin^2 2\theta_{13})/\sin^2 2\theta_{13}$ due to the degeneracy is plotted as a function of $\sin^2 2\theta_{23}$. Here, $\delta_{\text{de}}(\sin^2 2\theta_{13}) \equiv |\sin^2 2\theta_{13}' - \sin^2 2\theta_{13}|$ stands for the difference between the true solution $\sin^2 2\theta_{13}$ and the fake one $\sin^2 2\theta_{13}'$, and $\epsilon \equiv \Delta m_{21}^2/|\Delta m_{31}^2|$; $\epsilon = 6.9 \times 10^{-5}\,\text{eV}^2/2.5 \times 10^{-3}\,\text{eV}^2 = 0.028$ is for the best fit and an extreme case with $\epsilon = 1.9 \times 10^{-4}\,\text{eV}^2/1.6 \times 10^{-3}\,\text{eV}^2 = 0.12$, which is allowed at $90\,\%\,$CL (atmospheric) or $95\,\%\,$CL (solar), is also shown for illustration. The horizontal axis is suitably defined so that it is linear in $\sin^2 2\theta_{23}$, where the left half is for $\theta_{23} < \pi/4$ whereas the right half is for $\theta_{23} > \pi/4$. The solar mixing angle is taken as $\tan^2 \theta_{12} = 0.38$. $\sin^2 2\theta_{23} \geq 0.92$ has to be satisfied due to the constraint from the Super-Kamiokande atmospheric neutrino data. If the value of $\cos^2 2\theta_{23}$ is large enough, the value of $\delta_{\text{de}}(\sin^2 2\theta_{13})/\sin^2 2\theta_{13}$ increases and lies outside of the normalized error of the reactor experiment, then the reactor result may resolve the θ_{23} ambiguity.
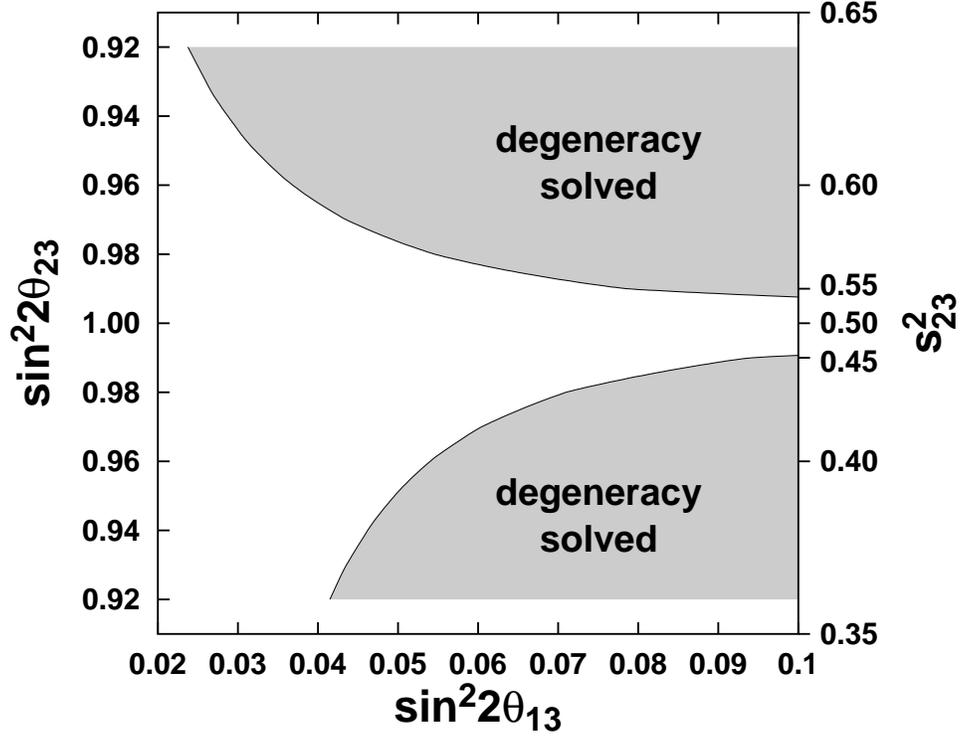
FIG. 7: The shadowed area stands for the region in which $\delta_{\mathrm{re}}(\sin^2 2\theta_{13}) < \delta_{\mathrm{de}}(\sin^2 2\theta_{13})$ is satisfied for σ_{sys}=0.8 %, 40 t·yr, d.o.f.=1 and for the best fit values of the solar and atmospheric oscillation parameters. In this shadowed region, the $(\theta_{13}, \theta_{23})$ degeneracy may be solved. The vertical axis is the same as the horizontal axis of Fig. 6(b).
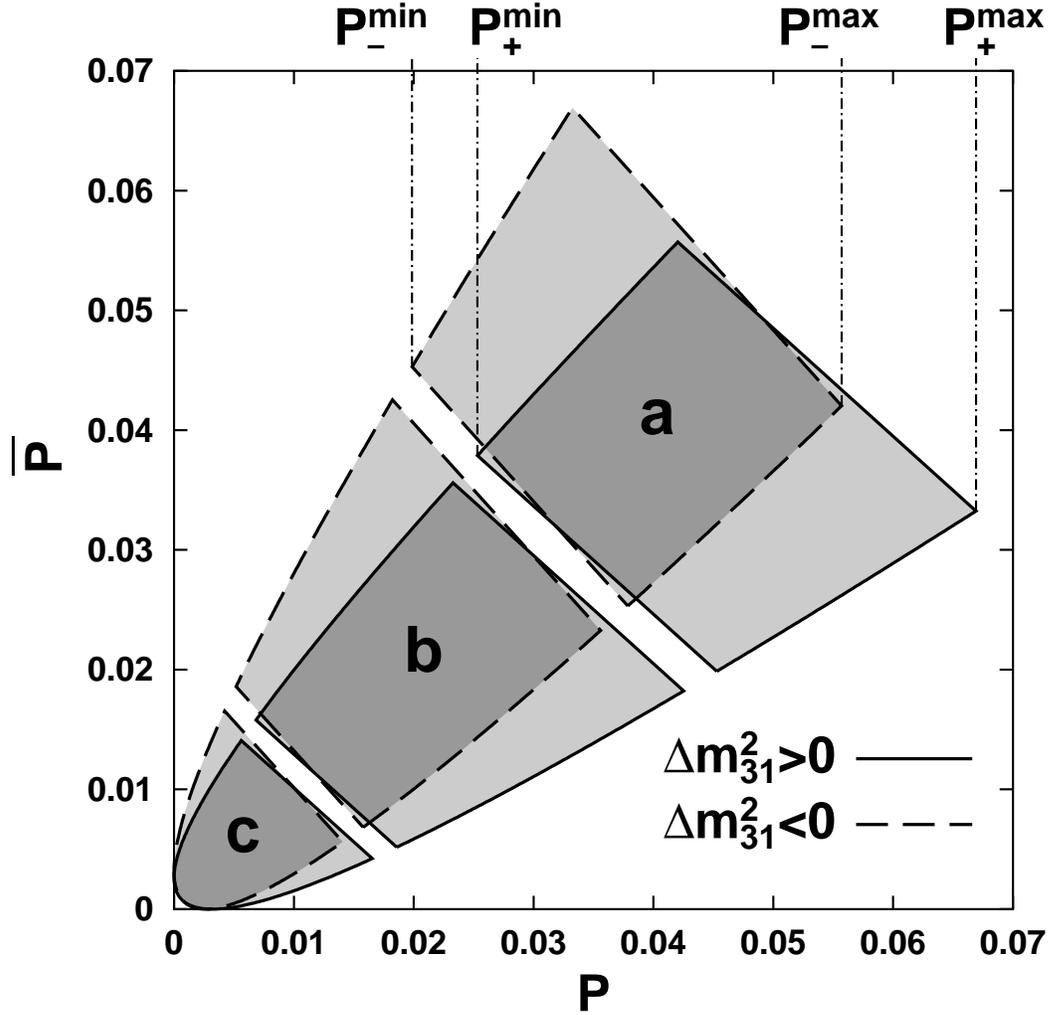
FIG. 8: Predicted allowed regions are depicted in the P–$\bar{P}$ plane for the JHF experiment at the oscillation maximum after an affirmative (a negative) result of the reactor experiment is obtained, where $P \equiv P(\nu_\mu \to \nu_e)$ and $\bar{P} \equiv P(\bar{\nu}_\mu \to \bar{\nu}_e)$ are the appearance probabilities, and $\theta_{23} = \pi/4$ is assumed. The cases a, b, c correspond to $\sin^2 2\theta_{13} = 0.08 \pm 0.018$, $\sin^2 2\theta_{13} = 0.04 \pm 0.018$, $\sin^2 2\theta_{13} < 0.019$, respectively. The regions bounded by the solid lines and the dashed lines are for the normal hierarchy ($\Delta m_{31}^2 > 0$) and the inverted hierarchy ($\Delta m_{31}^2 < 0$), respectively. Each region predicts the maximum ($P_\pm^{\max}$) and the minimum ($P_\pm^{\min}$) values of P for each hierarchy (+ for the normal and − for the inverted hierarchy), although $P_\pm^{\min}$ of the region c are zero.